Priority Brief

Cancer Immunology Research

Extracellular S100A9 Protein in Bone Marrow Supports Multiple Myeloma Survival by Stimulating Angiogenesis and Cytokine Secretion

Kim De Veirman[1], Nathan De Beule[1], Ken Maes[1], Eline Menu[1], Elke De Bruyne[1], Hendrik De Raeve[2], Karel Fostier[1], Jérôme Moreaux[3,4,5], Alboukadel Kassambara[3,4], Dirk Hose[6], Roy Heusschen[7], Helena Eriksson[8], Karin Vanderkerken[1], and Els Van Valckenborgh[1]

Abstract

Dysregulated expression of S100 protein family members is associated with cancer proliferation, invasion, angiogenesis, and inflammation. S100A9 induces myeloid-derived suppressor cell (MDSC) accumulation and activity. MDSCs, immunosuppressive cells that contribute to tumor immune escape, are the main producers of S100A9. In this study, we evaluated the role of extracellular S100A9 and the therapeutic relevance of S100A9 inhibition in multiple myeloma (MM), using the immunocompetent murine 5T33MM model. We demonstrated the presence of S100A9 and its receptor TLR4 in both monocytic and granulocytic MDSCs in human and mouse samples. We showed that S100A9 acted as a chemoattractant for MM cells and induced MDSCs to express and secrete inflammatory and pro-myeloma cytokines, including TNFα, IL6, and IL10. Blocking S100A9 interactions *in vivo* with the small molecule ABR-238901 did not directly affect MDSC accumulation but did reduce IL6 and IL10 cytokine expression by MDSC. ABR-238901 treatment *in vivo* reduced angiogenesis but had only minor effects on tumor load as single agent (6% reduction). However, ABR-238901 treatment in combination with bortezomib resulted in an increased reduction in tumor load compared with single treatments (50% relative reduction compared with bortezomib alone). Our data suggest that extracellular S100A9 promotes MM and that inhibition of S100A9 may have therapeutic benefit. *Cancer Immunol Res; 5(10); 839–46. ©2017 AACR.*

Introduction

Multiple myeloma (MM) is a hematologic cancer characterized by uncontrolled proliferation of plasma cells. The tumor cells localize preferentially to the bone marrow (BM), where the microenvironment promotes tumor cell survival and proliferation. The MM cells modulate the BM microenvironment resulting in angiogenesis, osteolytic lesions, anemia, and immunosuppression, leading to the clinical symptoms of MM disease (1). Although immunomodulatory agents, proteasome inhibitors, and monoclonal antibodies increase survival of MM patients (1), most patients relapse. New therapeutic approaches are needed.

S100A8 and S100A9 are calcium-binding proteins and mainly secreted by granulocytes and monocytes. Although S100A8 and S100A9 can form homodimers, their inflammatory properties derive from the heterodimer (S100A8/S100A9), which is also known as calprotectin. S100A9 is involved in many biological processes including inflammation, migration, invasion, and angiogenesis (2). Increased expression of S100A9, observed in several cancer types, including colorectal cancer and breast cancer, correlates with a bad prognosis (3, 4). Intracellular S100A9 signaling activates the NADPH oxidase complex resulting in increased reactive oxygen species (ROS) production, which in turn contributes to immunosuppression (5). Extracellular S100A9 protein can initiate the inflammatory cascade by interacting with the receptor for advanced glycation endproducts (RAGE) and Toll-like receptor 4 (TLR4). Subsequently, this activates the NFκB pathway, and inflammatory cytokines (including TNFα, IL1β, IL6, and IL8) are secreted (6). In solid tumors, S100A9 recruits MDSCs to the tumor site, resulting in immune suppression, increased tumor growth, and metastasis (7).

S100A9 knockout mice with MM show less MDSC accumulation and tumor growth in the BM compared with wild-type mice, correlating MDSC accumulation with MM progression (8). However, the use in that study of highly immunogenic OVA^+ MM cells might limit insight on the mechanisms by which S100A9 functions in MM development. Here, we investigated the role of extracellular S100A9 in MM using the immunocompetent 5T33MM mouse, in which MM progression is characterized by

[1]Department of Hematology and Immunology, Myeloma Center Brussels, Vrije Universiteit Brussel, Belgium. [2]Department of Pathology, UZ Brussel, Vrije Universiteit Brussel, Brussels, Belgium. [3]Department of Biological Hematology, CHU Montpellier, Montpellier, France. [4]Institute of Human Genetics, CNRS-UPR1142, Montpellier, France. [5]University of Montpellier, UFR de Médecine, Montpellier, France. [6]Medizinische Klinik, Universitätsklinikum Heidelberg, Heidelberg, Germany. [7]Laboratory of Hematology, GIGA-Research, University of Liège, Liège, Belgium. [8]Active Biotech AB, Lund, Sweden.

Note: Supplementary data for this article are available at Cancer Immunology Research Online (http://cancerimmunolres.aacrjournals.org/).

K. Vanderkerken and E. Van Valckenborgh contributed equally to this article.

Corresponding Author: Karin Vanderkerken, Vrije Universiteit Brussel, Laarbeeklaan 103, 1090 Brussels, Belgium. Phone: 32-2-629-21-08; Fax: 32-2-477-44-05; E-mail: karin.vanderkerken@vub.be

doi: 10.1158/2326-6066.CIR-17-0192

MDSC accumulation in the BM as well as increased angiogenesis. We studied the effect of ABR-238901, a small molecule that inhibits the interaction of S100A9 with its receptors. We investigated direct and indirect effects of S100A9 on MM cells, MDSCs, and angiogenesis.

Materials and Methods

Reagents

The S100A9 inhibiting compound ABR-238901 was kindly provided by Active Biotech AB. Bortezomib was obtained from Selleckchem. Recombinant S100A9 was obtained from R&D Systems.

Microarray data of human samples

Gene expression was investigated by the use of microarray data of the Heidelberg–Montpellier (HM) cohort including newly diagnosed MM patients and healthy volunteers (9–11). Expression of S100A9, TLR4, and RAGE was analyzed by Genomicscape (accession numbers E-MEXP-2360 and E-TABM-937). Gene expression data were normalized with the MAS5 algorithm. Normal BMPCs were derived from healthy controls, and other cell populations were obtained from MM patients.

Mice

C57BL/KaLwRij mice were purchased from Harlan CPB. They were housed and maintained following the conditions approved by the Ethical Committee for Animal Experiments, Vrije Universiteit Brussel (license no. LA1230281). The 5T33MM model originated from spontaneously developed MM in elderly C57BL/KalwRij mice and was propagated by intravenous transfer of the diseased marrow into young syngeneic mice (12). For *in vivo* experiments, mice were intravenously inoculated with 5×10^5 5T33MM cells.

Cell purification

Total BM was isolated from naïve and diseased 5T33MM mice followed by red blood cell lysis. Total MDSCs were positively selected by CD11b MACS beads (Miltenyi Biotec) according to the manufacturer's instructions. Granulocytic MDSCs were positively selected by Ly6G MACS beads (Miltenyi Biotec). The $Ly6G^-$ fraction was collected and further purified by the use of CD11b microbeads to obtain the monocytic MDSC population ($Ly6G^-CD11b^+$; purity > 90%). Cells were cultured in RPMI-1640 medium (Lonza) with 10% FCS (Biochrom AG) and supplements (100 U/mL penicillin/streptomycin and 2 mmol/L L-glutamine; Lonza).

Migration assay

Serum-free RPMI1640 medium (300 μL) containing recombinant S100A9 (5 μg/mL) was placed into a 24-well plate. A transwell insert (8 μmol/L pore size) was placed in each well and 5×10^4 5T33MMvv cells in 200 μL serum-free medium were added to the upper chamber. After 3 hours, cells that transmigrated into lower wells were collected and a known number of SpheroTM blank calibration beads (BD Biosciences) were added to cell suspensions as internal standard. Transmigrated cells were then counted with FACSCanto flow cytometer (Becton Dickinson).

Immunofluorescence staining

Cytospins were made at a concentration of 400,000 cells/mL and stored at −20°C). Cytopsins were fixed in 4% paraformaldehyde and washed with Tris–NaCl 0.05% Triton-X100 (Merck). Cytospins were blocked by 2% donkey serum and incubated overnight with the primary antibody to S100A9 (#AF2065, 10 μg/mL; R&D Systems). Next, cytospins were washed and incubated for 1 hour with donkey anti-goat-FITC (#AF488; R&D Systems). After washing, cytospins were mounted with Vectashield (Thermo Scientific) containing 4,6-diamidino-2-phenylindole (DAPI). Immunofluorescence was observed using a Nikon Eclipse 90i (Nikon France SAS).

Cell viability

Cell viability was determined by a CellTiter-Glo luminescent assay (Promega).

Western blot

Western blot was performed as described previously (13). S100A8 and S100A9 antibodies were purchased from R&D Systems. B-Actin was used as a loading control (Cell Signaling Technology). The pixel densities of proteins were quantified by ImageJ.

Flow cytometry

The following antibodies were used for murine samples: CD11b-FITC (Biolegend), Ly6G-PECy7 (Biolegend), CD8-FITC (Biolegend), IFNγ-PECy7 (Becton Dickinson), and isotype controls (Biolegend). Tumor load in the 5T33MM model was analyzed by the use of anti-idiotype (3H2), monoclonal antibody (IgG1), and APC-labeled rat anti-mouse IgG1 (secondary step; ref. 12). All antibodies for human samples were derived from Biolegend: CD11b-PECy7, CD33-PE, CD14-PB, CD15-PB, S100A9-APC, CD138-PE, and isotype controls.

T-cell proliferation assay

T cells were isolated from spleen of healthy mice followed by red blood cell lysis. Cells were stained by CFSE (0.1 μmol/L; Invitrogen) and resuspended in RPMI1640 medium supplemented with 10% HEPES (Sigma) and 20 μmol/L β-mercaptoethanol (Sigma). T cells were stimulated with 2 μL of CD3/CD28 Dynabeads (Invitrogen) and cultured for 3 days in the presence or absence of isolated $CD11b^+$ cells at different ratios. Cells were cultured in RPMI1640 medium (10% FCS) and proliferation was analyzed by flow cytometric CFSE dye dilution after CD3 staining.

ELISA

Supernatant was collected from $CD11b^+$ cells treated with recombinant S100A9 (5 μg/mL) for 24 hours and analyzed for IL6 and IL10 secretion by ELISA according to the manufacturer's instructions (eBioscience).

PCR

RNA was extracted by the RNeasy mini kit (Qiagen) and converted into cDNA using the first-strand cDNA synthesis kit (VWR International). Expression level of mRNA was quantified by qRT-PCR using ABI 7900TH Real-Time PCR System (Applied Biosystems). Primer sequences are listed in Supplementary Table S1 (Thermo Scientific).

Microvessel density

Microvessel density (MVD) was determined by CD31 staining. A femur was fixed in zinc fixative for 48 hours, followed by decalcification for 48 hours and embedded in paraffin. Paraffin sections were blocked with normal goat serum and incubated

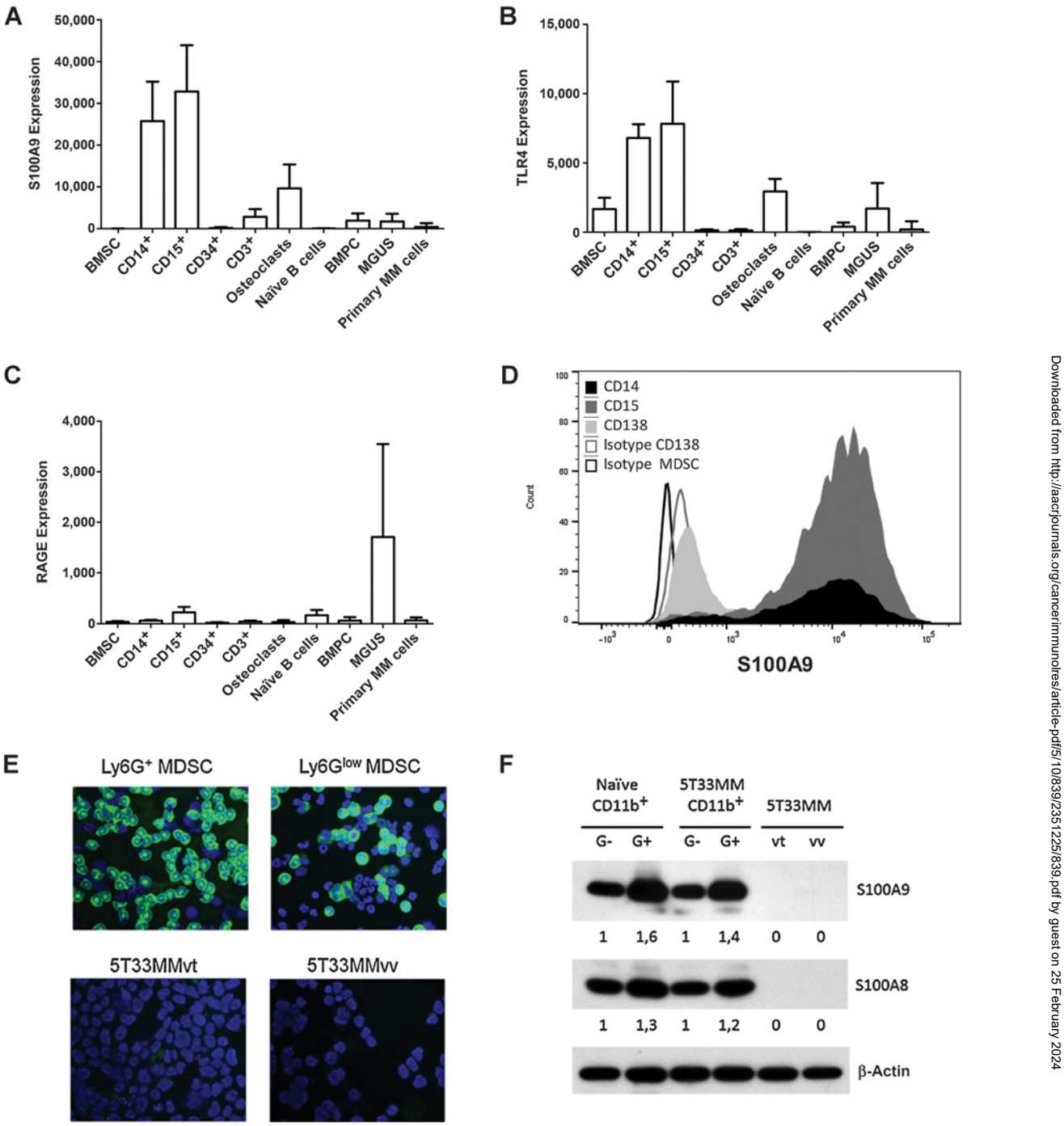

Figure 1.

S100A9, TLR4, and RAGE expression in multiple myeloma cells and myeloid cells. Gene expression was investigated by the use of microarray data of the Heidelberg–Montpellier (HM) cohort including newly diagnosed MM patients and healthy volunteers. S100A9 (**A**), TLR4 (**B**), and RAGE (**C**) expression was analyzed in bone marrow stromal cells (BMSC; $n = 5$), $CD14^+$ monocytic cells ($n = 5$), $CD15^+$ granulocytic cells ($n = 5$), $CD34^+$ hematopoietic cells ($n = 5$), $CD3^+$ T cells ($n = 5$), osteoclasts ($n = 7$), naïve B cells ($n = 5$), bone marrow plasma cells (BMPC; $n = 5$), MGUS ($n = 5$), and primary MM cells ($CD138^+$; $n = 206$). Bars represent mean ± standard deviation. **D,** S100A9 protein level was investigated by flow cytometry on BM samples of MM patients. MM cells ($CD138^+$), granulocytic MDSCs ($CD11b^+$ $CD33^+$ $CD15^+$), and monocytic MDSCs ($CD11b^+$, $CD33^+$, $CD14^+$) were costained for S100A9 and isotype controls were included. The result is representative of 5 independent experiments. **E,** Immunocytochemistry staining of S100A9 in 5T33MMvt cells (*in vitro* cell line), 5T33MMvv cells, $CD11b^+Ly6G^+$ granulocytic MDSCs, and $CD11b^+Ly6G^{low}$ monocytic MDSCs derived from 5T33MM diseased BM. One representative result of at least 3 independent experiments is shown. **F,** Western blot analysis of 5T33MMvt cells, 5T33MMvv cells, and $CD11b^+$ cells derived from naïve BM and 5T33MM-diseased BM. S100A8 and S100A9 expression were compared between monocytic MDSCs (G^-) and granulocytic MDSCs (G^+). One experiment representing three is shown.

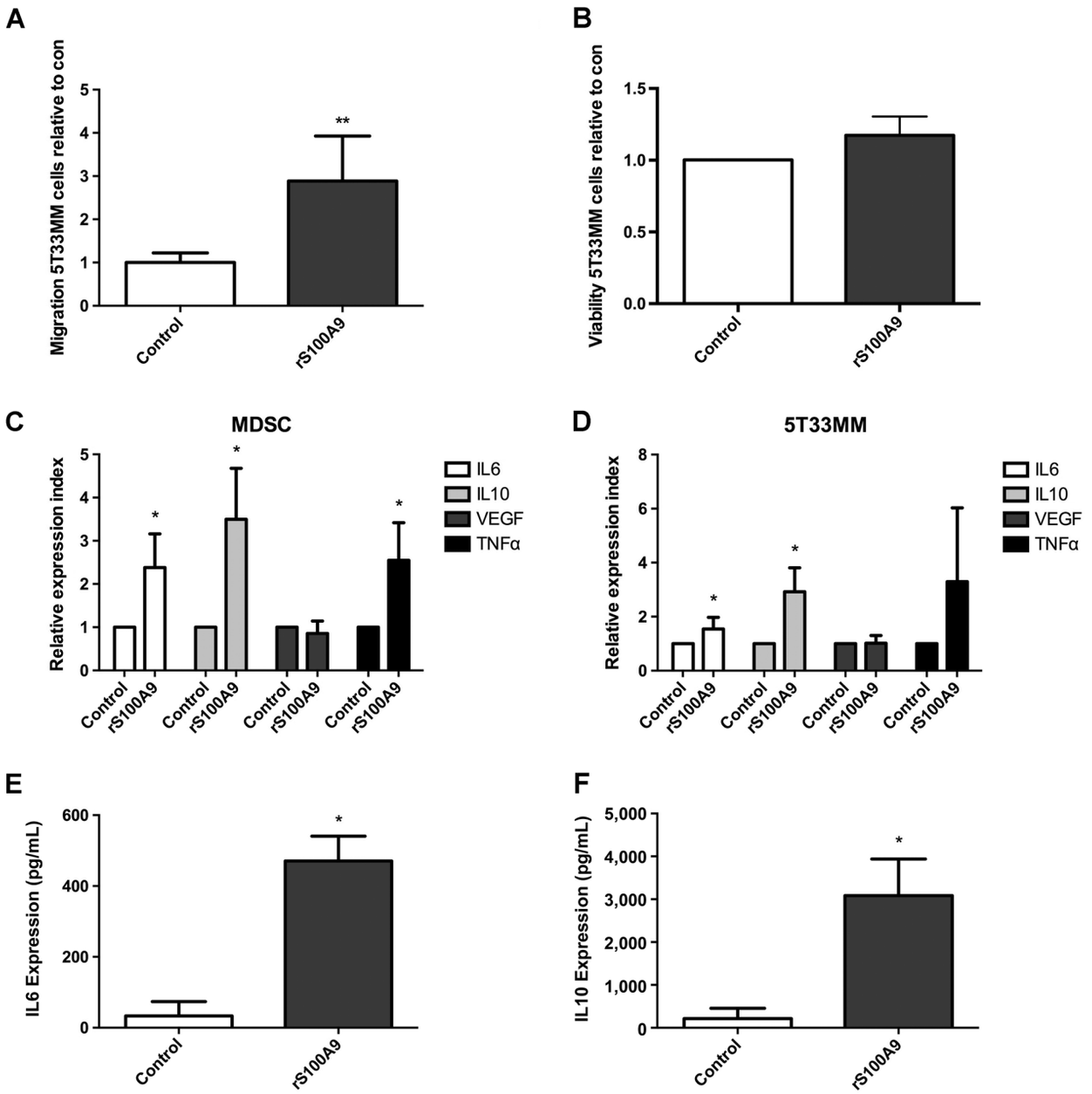

Figure 2.

Extracellular S100A9 regulates MM cell migration and proinflammatory cytokine secretion by myeloid-derived suppressor cells and MM cells. **A,** For the migration assay, recombinant S100A9 (5 μg/mL) was placed into the lower chamber and 5T33MMvv cells in the upper chamber. After 3 hours, cells that transmigrated into lower wells were collected and analyzed by FACSCanto flow cytometer ($n = 6$). **B,** 5T33MMvv cells were isolated and incubated with recombinant S100A9 (5 μg/mL) for 24 hours. Cell viability was determined by the use of a CellTiter-Glo luminescent assay ($n = 3$). **C** and **D,** MDSCs ($CD11b^+$) and 5T33MMvv cells ($CD11b^-$) were isolated from the BM of 5T33MM diseased mice and cultured with recombinant S100A9 (5 μg/mL) for 24 hours. mRNA expression levels of *IL6, IL10, TNFα*, and *VEGF* were analyzed by qRT-PCR ($n = 5$). **E** and **F,** Supernatant was collected from MDSCs treated with recombinant S100A9 (5 μg/mL) for 24 hours and analyzed for IL6 and IL10 secretion by ELISA ($n = 4$). For all graphs, bars represent mean ± standard deviation. *, $P < 0.05$; **, $P < 0.01$.

with a rat antibody to CD31 (PECAM-1, 1:10; PharMingen) overnight at 4°C. A biotin-conjugated goat anti-rat IgG was used as a secondary antibody (1:75; PharMingen). A streptavidin–horseradish peroxidase conjugate in combination with tyramide signal amplification (TSA; NEN Life Science Products) was used for detection. The number of blood vessels in the area with the highest blood vessel density was counted per 0.22 mm^2.

Statistical analysis

Statistical analysis was done using GraphPad Prism 5 software. Results were analyzed using the Mann–Whitney *U* test

and one-way ANOVA test. $P < 0.05$ (*), $P < 0.01$ (**), and $P < 0.001$ (***) were considered statistically significant. To determine sample size for *in vivo* experiments we used G-power (3.1). Wilcoxon–Mann–Whitney test was used to compare two independent groups. *F*-test one-way ANOVA was used to compare multiple groups. Details of the power analysis were included supplementary.

Results and Discussion

Expression of *S100A9*, *TLR4*, and *RAGE* genes was investigated in cell populations from MM patients. We studied BM hematopoietic stem cells ($CD34^+$), T lymphocytes ($CD3^+$), monocytes ($CD14^+$), polymorphonuclear neutrophils ($CD15^+$), *in vitro* generated osteoclasts, BM stromal cells (BMSC), BM plasma cells (BMPC), naïve B cells ($CD19^+$), and primary MM cells (MMC). RNA expression of *S100A9* and its receptor *TLR4* was observed in $CD14^+$ monocytic and $CD15^+$ granulocytic myeloid cells derived from MM patients (Fig. 1A and B). RNA expression of *RAGE* had the lowest signal intensity (Fig. 1C). *S100A9* expression was less in primary MM cells than in BMPC and MGUS (Fig. 1A). Flow cytometry staining confirmed S100A9 protein presence in $CD14^+$ and $CD15^+$ cells but not in human $CD138^+$ myeloma cells (Fig. 1D). The murine 5T33MM model, as with the human disease, displays monoclonal immunoglobulin (M protein) producing MM cells localized in the BM, increased angiogenesis and increased presence (>10% increase in the 5T33MM model compared with naïve mice) and immunosuppressive activity of MDSCs (14, 15). Immunostaining and Western blot analysis showed S100A9 in granulocytic ($Ly6G^+$) and monocytic ($Ly6G^{low}$) MDSCs isolated from 5T33MM-diseased mice with more S100A9 in granulocytic MDSCs than in monocytic MDSCs (Fig. 1E and F). S100A9 protein was undetectable in 5T33MM cells from *in vitro* cultures (5T33MMvt) or purified from the BM of diseased mice (5T33MMvv; Fig. 1E and F). Furthermore, S100A9 expression was not different between normal and MM myeloid cells. S100A8, which forms heterodimers with S100A9, had a similar expression profile (Fig. 1F). This is in concordance with a previous study in colon cancer in which S100A9 protein concentrations were similar in $Gr\text{-}1^+$ cells from naïve and tumor-bearing mice (5). S100A9 protein levels in tumor cells are mostly studied in solid cancers and variable expression has been noticed in different types of tumors (3, 4). We found that MM cells do not produce S100A9 protein, and myeloid cells are the main source of S100A9 protein. S100A9 functions intracellularly (8), but can also be released extracellularly by cell damage or death, or can be actively secreted by myeloid cells at sites of inflammation (16). These data impelled us to study the role of extracellular S100A9 in MM disease.

We investigated the effect of recombinant S100A9 on migration and viability of myeloma cells *in vitro*. Recombinant S100A9 increased the migration of 5T33MMvv cells (Fig. 2A) but did not affect cell viability after incubation for 24 hours (Fig. 2B). S100A9 also induces cytokine release (6). Therefore, the effect of recombinant S100A9 on cytokine expression in 5T33MMvv cells and MDSCs was investigated by qRT-PCR. In both cell populations, S100A9 could induce expression of *IL6*, *IL10*, and *TNFα*, all of which promote proliferation and survival of MM cells (Fig. 2C and D). By ELISA, we confirmed the S100A9-mediated release of IL6 and IL10 by MDSCs (Fig. 2E and F). IL6 plays an essential role

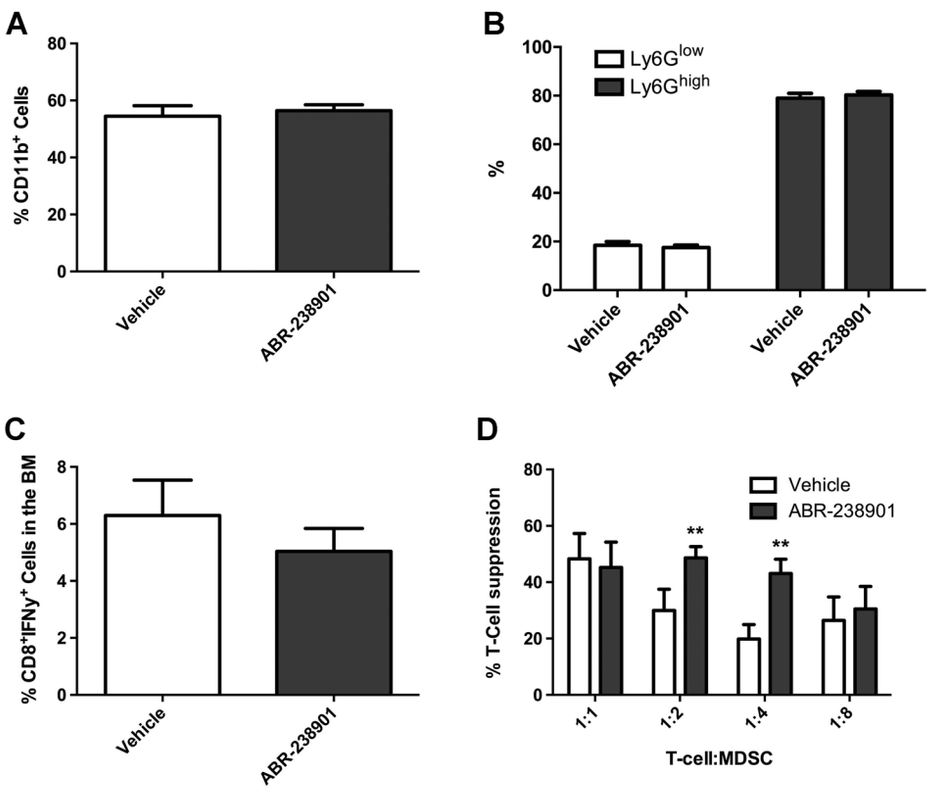

Figure 3.

The effect of S100A9 inhibitors on MDSCs *in vivo*. 5T33MM-inoculated mice (0.5×10^6 cells/mouse, intravenously) were treated at day 1 with vehicle or ABR-238901 (30 mg/kg, gavage, daily) for 5 days ($n = 5$/group). After treatment, BM cells were isolated and flow cytometry for CD11b (**A**), Ly6G (**B**), CD8, and IFNγ (**C**) was performed. **D,** $CD11b^+$ MDSCs were purified and cocultured with CFSE-labeled T cells at indicated ratios. T-cell proliferation was analyzed after 72 hours ($n = 5$). A power analysis (see Supplementary Information) was performed for these experiments to determine the minimum number of animals in one experiment that are necessary to retain sufficient statistical power, when each mouse is considered an independent repetition of the experiment. In all graphs, bars represent mean ± standard deviation. **, $P < 0.01$.

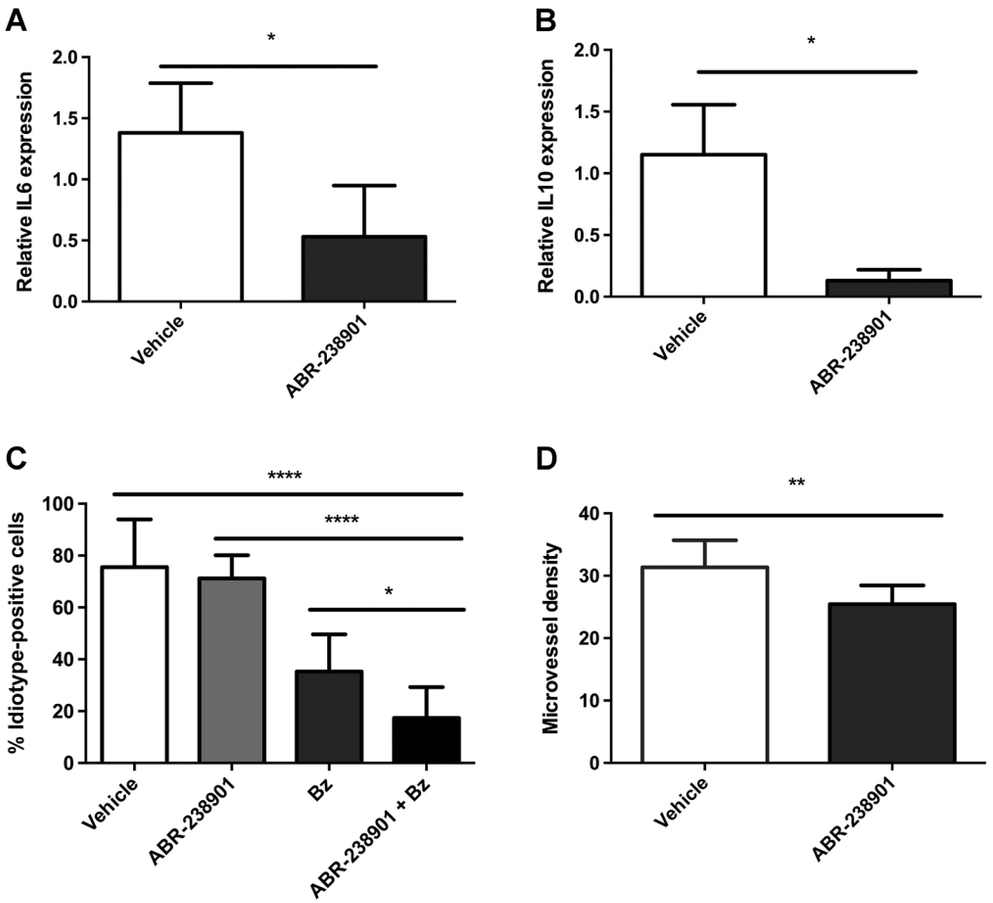

Figure 4.

The effect of S100A9 inhibition on cytokine expression and MM tumor load *in vivo*. C57BL/KaLwRij mice were inoculated with 5T33MMvv cells. One day later, mice were treated with the S100A9 inhibitor ABR-238901 (daily gavage, 30 mg/kg, $n = 10$). **A** and **B,** $CD11b^+$ cells were purified and analyzed for *IL6* and *IL10* cytokine expression by qRT-PCR. **C,** Tumor load was assessed by flow cytometry for idiotype. **D,** 5T33MM inoculated mice were treated 1 day after tumor-cell injection with ABR-238901 (daily gavage, 30 mg/kg, $n = 10$) in combination with bortezomib (0.6 mg/kg subcutaneously, 2 times/week). Tumor load was assessed by flow cytometry for idiotype. **D,** 5T33MM inoculated mice were treated with ABR-238901 (daily gavage, 30 mg/kg, $n = 10$). Microvessel density (MVD) was determined by CD31 staining on BM sections. A power analysis (see Supplementary Information) was performed for these experiments to determine the minimum number of animals in one experiment that are necessary to retain sufficient statistical power, when each mouse is considered an independent repetition of the experiment. For all graphs, bars represent mean ± standard deviation. *, $P < 0.05$; **, $P < 0.01$; ****, $P < 0.0001$.

in MM pathogenesis as it is the most important growth and survival factor for myeloma cells. IL6 also interacts with adhesion molecules, oncogenes, and tumor suppressor genes (17). IL10 is a potent IL6-independent growth factor for MM cells (18). Our data are in agreement with studies where S100A9 treatment was linked to pro-inflammatory responses by activation of the NFκB and MAPK signaling pathways (6). In addition, Gao and colleagues observed S100A9-induced release of IL6 and IL8 through TLR4 interaction in human periodontal ligament cells (19).

To investigate the role of S100A9 in MM *in vivo*, the small molecule ABR-238901 ([a (heteroaryl)-sulfonamide derivative], which inhibits interactions between S100A9 and its receptor, was used in the 5T33MM mouse model. MDSC populations express high levels of S100A9 and its receptors, so we first investigated the direct effect of ABR-238901 on MDSC accumulation and immunosuppressive activity after *in vivo* treatment. As MDSCs accumulate 1 week after MM cell inoculation into mice (14), ABR-238901 treatment was started at day 1 after MM cell injection and treatment was given for 5 days. Treated and untreated mice had similar percentages of $CD11b^+$ MDSCs, monocytic ($Ly6G^{low}$) and granulocytic ($Ly6G^{high}$) MDSC subpopulations, and $IFNy^+$ $CD8^+$ T cells (Fig. 3A–C). In addition, MDSCs from treated and untreated mice were cocultured with anti-CD3/CD28 stimulated T cells, and T-cell proliferation was measured after 3 days. Blocking S100A9 interactions *in vivo* did not block the T-cell–suppressive activity of MDSC; on the contrary, ABR-238901 treatment induced the suppressive activity of MDSCs (Fig. 3D). Neither viability nor apoptosis was changed *in vitro* when incubating the compound ABR-238901 with $CD11b^+$ MDSCs from diseased mice (Supplementary Fig. S1). Thus, extracellular and intracellular S100A9 have different functions, as S100A9 protein–knockout mice have less MDSC accumulation and, as result, more antigen-specific $CD8^+$ T cells in immunocompetent DP42-OVA MM models (8). Different solid tumors show that S100A9 inhibitors

reduce MDSC accumulation and induce immune responses, mainly by blocking migration of MDSCs toward the tumor. However, in MM, MDSCs are already present at the tumor in the BM and so the consequences of S100A9 inhibitors on MDSC migration can be limited.

Next, we evaluated cytokine expression in MDSCs and MM cells isolated from mice treated either with ABR-238901 or vehicle. 5T33MM mice were treated with ABR-238901 for 3 weeks, and BM was isolated from mice to purify MDSCs ($CD11b^+$) and MM ($CD11b^-$) cells by MACS and analyze *IL6* and *IL10* expression by *qRT-PCR*. Less IL6 and IL10 was observed in MDSCs from ABR-238901 treated mice compared with vehicle-treated mice (Fig. 4A and B). In addition, we observed less *IL10* expression in the MM cells, although *IL6* expression was unaffected (Supplementary Fig. S2). These results indicate that S100A9 expression by myeloid cells leads to the secretion of proinflammatory cytokines (e.g., IL6 and IL10) in MDSCs and tumor cells and therefore contributes to a favorable microenvironment for MM cell growth.

In MM, limited success is achieved with single-agent therapy. From large randomized trials in MM patients, we know that combination therapy produces longer progression-free survival than does single therapy both in newly diagnosed and relapsed patients (20). Thus, we evaluated the combination of the clinically used anti-MM agent bortezomib together with ABR-238901 in the 5T33MM model. ABR-238901 in combination with bortezomib resulted in reduced tumor load compared with treatments of either agent alone (Fig. 4C). As with human MM, angiogenesis, which supports MM cell growth and survival, is induced in the 5T33MM model (21). Granulocytic MDSC, here described as the main producers of S100A9, also exert a proangiogenic role in MM (22). Therefore, to investigate whether S100A9 is involved in angiogenesis, mice were treated with ABR-238901 for 3 weeks and analyzed for BM microvessel density using CD31 immunostainings. Less angiogenesis was observed in 5T33MM mice treated with ABR-238901 compared with 5T33MM mice treated with vehicle (Fig. 4D). Low concentrations of S100A8/A9 promote neovascularization by the increase in proliferation, migration, and tube formation of human umbilical vascular endothelial cells and S100A8/S100A9 proteins thus serve as proangiogenic factors causing increased blood supply and subsequently tumor progression (23). The S100A9–receptor interaction is also inhibited by quinoline-3-carboxamide analogs including tasquinimod and paquinimod. Tasquinimod, administered orally in a phase III clinical trial in metastatic castration-resistant prostate cancer, increased progression-free survival but not overall survival when compared with placebo (24). In MM, tasquinimod-treatment resulted in reduced tumor load and reduced angiogenesis in xenograft MM models. S100A9KO mice treated with tasquinimod did not show improved survival compared with vehicle group, indicating that the antitumor effect was mediated by selective targeting of S100A9 and not by a direct antitumor effect (25).

We conclude that S100A9, mainly produced by myeloid cells in the BM, is involved in the pathogenesis of MM. S100A9 attracted MM cells to the BM where it provided a survival niche by inducing the growth factors IL6 and IL10, as well as promoting angiogenesis. We found that a combination therapy that used bortezomib along with an agent to block S100A9 interactions reduced tumor load *in vivo*. Such a combination may have therapeutic relevance in the treatment of MM patients.

Disclosure of Potential Conflicts of Interest

H. Eriksson is Head of BioScience at Active Biotech AB and has ownership interest in Active Biotech AB. No potential conflicts of interest were disclosed by the authors.

Authors' Contributions

Conception and design: K. De Veirman, D. Hose, K. Vanderkerken, E. Van Valckenborgh

Development of methodology: K. De Veirman, N. De Beule, H. De Raeve

Acquisition of data (provided animals, acquired and managed patients, provided facilities, etc.): K. De Veirman, N. De Beule, H. De Raeve, K. Fostier, J. Moreaux, D. Hose, R. Heusschen, E. Van Valckenborgh

Analysis and interpretation of data (e.g., statistical analysis, biostatistics, computational analysis): K. De Veirman, N. De Beule, H. De Raeve, A. Kassambara, D. Hose, R. Heusschen, E. Van Valckenborgh

Writing, review, and/or revision of the manuscript: K. De Veirman, N. De Beule, K. Maes, E. Menu, E. De Bruyne, K. Fostier, J. Moreaux, D. Hose, H. Eriksson, K. Vanderkerken, E. Van Valckenborgh

Administrative, technical, or material support (i.e., reporting or organizing data, constructing databases): K. De Veirman, N. De Beule

Study supervision: K. Vanderkerken, E. Van Valckenborgh

Acknowledgments

The authors would like to thank Carine Seynaeve and Sofie Seghers for excellent technical assistance.

Grant Support

This work was supported by the SRP-VUB, Universitaire Stichting van België, and Wetenschappelijk Fonds Willy Gepts of the UZ Brussel and in part by the German Federal Ministry of Education ["CLIOMMICS" (01ZX1309) and "CAMPSIMM" (01ES1103)] and the Deutsche Forschungsgemeinschaft (SFB/TRR79, subprojects B12, B1 and M9). Nathan De Beule is a PhD student and Kim De Veirman, Elke De Bruyne, and Ken Maes are postdoctoral fellows of FWO-VI.

Received April 13, 2017; revised July 12, 2017; accepted August 30, 2017; published OnlineFirst September 13, 2017.

References

1. Anderson KC. Progress and paradigms in multiple myeloma. Clin Cancer Res 2016;22:5419–27.
2. Srikrishna G. S100A8 and S100A9: new insights into their roles in malignancy. J Innate Immun 2012;4:31–40.
3. Arai K, Takano S, Teratani T, Ito Y, Yamada T, Nozawa R. S100A8 and S100A9 overexpression is associated with poor pathological parameters in invasive ductal carcinoma of the breast. Curr Cancer Drug Targets 2008;8:243–52.
4. Duan L, Wu R, Ye L, Wang H, Yang X, Zhang Y, et al. S100A8 and S100A9 are associated with colorectal carcinoma progression and contribute to colorectal carcinoma cell survival and migration via Wnt/β-catenin pathway. PLoS One 2013;8:e62092.
5. Cheng P, Corzo CA, Luetteke N, Yu B, Nagaraj S, Bui MM, et al. Inhibition of dendritic cell differentiation and accumulation of myeloid-derived suppressor cells in cancer is regulated by S100A9 protein. J Exp Med 2008;205:2235–49.
6. Sunahori K, Yamamura M, Yamana J, Takasugi K, Kawashima M, Yamamoto H, et al. The S100A8/A9 heterodimer amplifies proinflammatory cytokine production by macrophages via activation of nuclear factor kappa

B and p38 mitogen-activated protein kinase in rheumatoid arthritis. Arthritis Res Ther 2006;8:R69.
7. Sinha P, Okoro C, Foell D, Freeze HH, Ostrand-Rosenberg S, Srikrishna G. Proinflammatory S100 proteins regulate the accumulation of myeloid-derived suppressor cells. J Immunol 2008;181:4666–75.
8. Ramachandran IR, Martner A, Pisklakova A, Condamine T, Chase T, Vogl T, et al. Myeloid-derived suppressor cells regulate growth of multiple myeloma by inhibiting T cells in bone marrow. J Immunol 2013;190:3815–23.
9. Kassambara A, Rème T, Jourdan M, Fest T, Hose D, Tarte K, et al. GenomicScape: an easy-to-use web tool for gene expression data analysis. Application to investigate the molecular events in the differentiation of B Cells into plasma cells. PLoS Comput Biol 2015;11:e1004077.
10. Moreaux J, Hose D, Kassambara A, Rème T, Moine P, Requirand G, et al. Osteoclast-gene expression profiling reveals osteoclast-derived CCR2 chemokines promoting myeloma cell migration. Blood 2011;117:1280–90.
11. Seckinger A, Meissner T, Moreaux J, Depeweg D, Hillengass J, Hose K, et al. Clinical and prognostic role of annexin A2 in multiple myeloma. Blood 2012;120:1087–94.
12. Vanderkerken K, De Raeve H, Goes E, Van Meirvenne S, Radl J, Van Riet I, et al. Organ involvement and phenotypic adhesion profile of 5T2 and 5T33 myeloma cells in the C57BL/KaLwRij mouse. Br J Cancer 1997;76:451–60.
13. De Bruyne E, Bos TJ, Schuit F, Van Valckenborgh E, Menu E, Thorrez L, et al. IGF-1 suppresses Bim expression in multiple myeloma via epigenetic and posttranslational mechanisms. Blood 2010;115:2430–40.
14. De Veirman K, Van Ginderachter JA, Lub S, De Beule N, Thielemans K, Bautmans I, et al. Multiple myeloma induces Mcl-1 expression and survival of myeloid-derived suppressor cells. Oncotarget 2015;6:10532–47.
15. Van Valckenborgh E, Schouppe E, Movahedi K, De Bruyne E, Menu E, De Baetselier P, et al. Multiple myeloma induces the immunosuppressive capacity of distinct myeloid-derived suppressor cell subpopulations in the bone marrow. Leukemia 2012;26:2424–8.
16. Foell D, Wittkowski H, Vogl T, Roth J. S100 proteins expressed in phagocytes: a novel group of damage-associated molecular pattern molecules. J Leukoc Biol 2007;81:28–37.
17. Gadó K, Domján G, Hegyesi H, Falus A. Role of interleukin-6 in the pathogenesis of multiple myeloma. Cell Biol Int 2000;24:195–209.
18. Gu ZJ, Costes V, Lu ZY, Zhang XG, Pitard V, Moreau JF, et al. Interleukin-10 is a growth factor for human myeloma cells by induction of an oncostatin M autocrine loop. Blood 1996;88:3972–86.
19. Gao H, Zhang X, Zheng Y, Peng L, Hou J, Meng H. S100A9-induced release of interleukin (IL)-6 and IL-8 through toll-like receptor 4 (TLR4) in human periodontal ligament cells. Mol Immunol 2015;67:223–32.
20. Lonial S, Kaufman JL. The era of combination therapy in myeloma. J Clin Oncol 2012;30:2434–6.
21. Van Valckenborgh E, De Raeve H, Devy L, Blacher S, Munaut C, Noël A, et al. Murine 5T multiple myeloma cells induce angiogenesis in vitro and in vivo. Br J Cancer 2002;86:796–802.
22. Binsfeld M, Muller J, Lamour V, De Veirman K, De Raeve H, Bellahcène A, et al. Granulocytic myeloid-derived suppressor cells promote angiogenesis in the context of multiple myeloma. Oncotarget 2016; 7:37931–43.
23. Li C, Li S, Jia C, Yang L, Song Z, Wang Y. Low concentration of S100A8/9 promotes angiogenesis-related activity of vascular endothelial cells: bridges among inflammation, angiogenesis, and tumorigenesis? Mediators Inflamm 2012;2012:248574.
24. Sternberg C, Armstrong A, Pili R, Ng S, Huddart R, Agarwal N, et al. Randomized, double-blind, placebo-controlled phase III study of tasquinimod in men with metastatic castration-resistant prostate cancer. J of Clin Oncol 2016;34:2636–43.
25. Ramachandran IR, Lin C, Chase T, Gabrilovich D, Nefedova Y. A novel agent tasquinimod demonstrates a potent anti-tumor activity in preclinical models of multiple myeloma. Blood 2014;124:5729.